

# Nontrivial topology of the Alfvén continuum and topological character of reversed-shear Alfvén eigenmodes

Jeffrey B. Parker\*

*Lawrence Livermore National Laboratory, Livermore, CA 94550, USA*

J. W. Burby

*Los Alamos National Laboratory, Los Alamos, NM 87545, USA*

J. B. Marston

*Brown Center for Theoretical Physics, Box S, Brown University, Providence, RI 02912, USA*

Steven M. Tobias

*Department of Applied Mathematics, University of Leeds, Leeds, LS2 9JT, United Kingdom*

In an inhomogeneous plasma, the ideal magnetohydrodynamics model gives rise to the Alfvén continuum, consisting of non-square-integrable improper eigenfunctions. For a gravitating slab, we calculate a Chern number for the Alfvén continuum on a given magnetic surface. For strong magnetic shear, the Chern number is equal to  $\pm 1$ , depending on the sign of the shear. By appeal to the bulk-boundary correspondence, this result suggests a topological character of the reversed-shear Alfvén eigenmode, which has been observed in tokamaks and is radially localized to layers of zero magnetic shear. As a result, the reversed-shear Alfvén eigenmode may be topologically robust to three-dimensional perturbations such as magnetic islands.

## INTRODUCTION

Recent discoveries have demonstrated the fundamental importance of topology and topological phase to qualitative understanding of physical systems [1]. An important feature in topological understanding is the bulk-boundary correspondence principle: the boundary between two materials with differing topological phase has associated interface modes. This effect has been observed in electronic [1], photonic [2], acoustic [3, 4], mechanical [5], and fluid [6, 7] systems. The interface modes have attracted significant interest in enabling more efficient devices due to topological protection, the tendency to be robust against scattering in the presence of defects. Applied to plasma systems such as fusion devices, topology offers a profound window into wave physics.

A tokamak is a toroidal device used to magnetically confine hot plasma for the purpose of controlled nuclear fusion. The ideal magnetohydrodynamics (MHD) equilibrium of a tokamak consists of a set of nested torii, in which each torus, labeled by a radial coordinate  $\psi$ , forms a magnetic surface where the magnetic field lies within each surface. The magnetic field structure can be characterized by a helical measure, called the safety factor  $q(\psi)$ , which is proportional to the ratio of toroidal and poloidal field strengths and depends only on  $\psi$ . The magnetic shear is proportional to  $dq/d\psi$ .

A class of modes known as reversed-shear Alfvén eigenmodes (RSAEs) [8–11] has been observed in multiple tokamaks [12–20] and at least one stellarator [21]. The RSAEs are radially localized to regions of zero magnetic shear, at an extremum of  $q(\psi)$ . RSAEs are an MHD-

type mode, and can be excited by kinetic effects such as resonance with energetic particles. A concern for future fusion devices such as ITER is how the interaction between particles and Alfvén eigenmodes may limit reactor performance [22–25]. On the other hand, RSAEs have also proven useful for MHD spectroscopy [26], as they can be reliably detected, with oscillation frequency close to that predicted by linear theory [27–29]. Detection of the RSAEs can provide information about the magnetic field and safety factor that may be difficult to obtain by other means.

In this letter, we reconsider RSAEs from a topological perspective. The Chern number is a topological invariant that characterizes the band structure of a system and can be calculated by integrating the Berry curvature, an eigenfunction-dependent quantity, over momentum space. Using a sheared-slab geometry, we investigate a means of assigning Chern numbers to the Alfvén continuum. The Alfvén continuum is associated with non-square-integrable improper eigenfunctions. An important question is whether a topological characterization of a substance and the bulk-boundary correspondence are applicable to such improper eigenfunctions. We develop a procedure to compute Chern numbers for the improper eigenfunctions by using regularization. We find that the Chern number depends on the sign of the magnetic shear. Hence, bulk-boundary correspondence implies that the change in topological phase is linked to a wave existing at the interface where the shear vanishes.

While the Alfvén spectrum becomes more complicated in toroidal geometry, the Alfvén continuum and improper eigenfunctions continue to exist in modified form. Therefore, the RSAE may have topological character. This re-

sult may also shed light on solar physics, where Alfvén waves can likewise play an important role [30, 31].

*Linear ideal MHD* We consider a gravitating slab in ideal MHD equilibrium, where equilibrium quantities depend only on  $x$ . The acceleration due to gravity is  $-\hat{g}\hat{\mathbf{x}}$ , where  $\hat{g}$  is a constant. The gravitational force here plays a role fulfilled by magnetic curvature in toroidal geometry. The equilibrium magnetic field is  $\mathbf{B}(x) = B_y(x)\hat{\mathbf{y}} + B_z(x)\hat{\mathbf{z}}$ . Perturbing about the equilibrium, we obtain the standard linearized ideal MHD formulation,  $\rho\partial^2\boldsymbol{\xi}/\partial t^2 = \mathbf{F}(\boldsymbol{\xi})$ , where  $\boldsymbol{\xi}$  is the fluid displacement vector,  $\rho$  is the equilibrium mass density, and  $\mathbf{F}$  is the self-adjoint force operator. After a Fourier transform in time, this problem has self-adjoint form with eigenvalue  $\omega^2$ . In what follows, we use the low-plasma-beta limit to neglect the slow magnetosonic wave and isolate the Alfvén continuum.

Assuming that modes have dependence  $\sim e^{i(k_y y + k_z z - \omega t)}$ , we obtain the wave equation for the three components of  $\boldsymbol{\xi}$ , taken here as  $\xi \stackrel{\text{def}}{=} \boldsymbol{\xi} \cdot \hat{\mathbf{x}}$ ,  $\eta \stackrel{\text{def}}{=} i\boldsymbol{\xi} \cdot \hat{\mathbf{e}}_\perp$ , and  $\zeta \stackrel{\text{def}}{=} i\boldsymbol{\xi} \cdot \hat{\mathbf{b}}$ , and we have defined  $\hat{\mathbf{b}} \stackrel{\text{def}}{=} \mathbf{B}/B$  and  $\hat{\mathbf{e}}_\perp \stackrel{\text{def}}{=} \hat{\mathbf{b}} \times \hat{\mathbf{x}}$ . The wave equation is [32]

$$-\rho\omega^2\xi = (\rho b^2\xi')' - \rho f^2 b^2\xi + (\rho g b^2\eta)' + \rho g\hat{g}\eta + \rho f\hat{g}\zeta, \quad (1a)$$

$$-\rho\omega^2\eta = -\rho g b^2\xi' + \rho g\hat{g}\xi - \rho(f^2 + g^2)b^2\eta, \quad (1b)$$

$$-\rho\omega^2\zeta = \rho f\hat{g}\xi, \quad (1c)$$

where a prime denotes derivative with respect to  $x$ ,  $f \stackrel{\text{def}}{=} (k_y B_y + k_z B_z)/B$  and  $g \stackrel{\text{def}}{=} (k_y B_z - k_z B_y)/B$  are the parallel and the signed perpendicular wavenumbers, and  $b^2 \stackrel{\text{def}}{=} B^2/\rho$  is the Alfvén speed squared ( $b^2$  is to be distinguished from the unit vector  $\hat{\mathbf{b}}$ ). The permeability  $\mu_0$  has been set to 1. One can solve for  $\eta$  and  $\zeta$  in terms of  $\xi$ , as  $\eta = g[\omega^2 - (f^2 + g^2)b^2]^{-1}(b^2\xi' - \hat{g}\xi)$  and  $\zeta = -(f\hat{g}/\omega^2)\xi$ .

One then obtains a single equation for  $\xi$  [32],

$$\frac{d}{dx} \left( P \frac{d\xi}{dx} \right) - Q\xi = 0, \quad (2)$$

where  $P \stackrel{\text{def}}{=} \rho b^2 \omega^2 (\omega^2 - \omega_A^2)/D$ ,  $Q \stackrel{\text{def}}{=} -\rho(\omega^2 - \omega_A^2) - \rho'\hat{g} + \rho(f^2 + g^2)\hat{g}^2(\omega^2 - \omega_A^2)/D + [\rho\hat{g}\omega^2(\omega^2 - \omega_A^2)/D]'$ ,  $D \stackrel{\text{def}}{=} \omega^2[\omega^2 - (f^2 + g^2)b^2]$ , and  $\omega_A^2 \stackrel{\text{def}}{=} f^2 b^2$  is the local Alfvén frequency. For any  $x_0$ ,  $k_y$ , and  $k_z$ , there is a solution with frequency  $\omega^2 = \omega_A^2(x_0, k_y, k_z)$ , which leads to the Alfvén continuum. At that frequency,  $P(x_0) = 0$ , and  $x_0$  is a regular singular point of Eq. (2). Let  $s \stackrel{\text{def}}{=} x - x_0$ . For  $(\omega_A^2)'_0 \neq 0$  (a subscript denotes evaluation at  $s = 0$ ), a Frobenius series expansion for  $\xi$  about  $s = 0$  results in a repeated indicial exponent of zero, implying there are two solutions,

$$\xi_1 = u(s) \quad (3)$$

$$\xi_2 = u(s) \ln s + v(s) \quad (4)$$

where  $u(s)$  and  $v(s)$  have a Taylor series. The logarithmic singularity of  $\xi_2$  is square integrable, but  $\eta_2$ , which depends on  $\xi_2'$ , is not.

In the series  $u(s) = 1 + u_1 s + \dots$ , we find

$$u_1 = u_{1a} + \frac{\hat{g}}{b_0^2}, \quad (5)$$

where  $u_{1a} \stackrel{\text{def}}{=} g_0^2 Q_{0a}/\rho_0(\omega_A^2)'_0$  and  $Q_{0a} \stackrel{\text{def}}{=} -\rho'_0 \hat{g}$ . We have split off  $u_{1a}$  because it plays an important role while the other term will cancel out.

The  $|\psi\rangle \stackrel{\text{def}}{=} [\xi_2, \eta_2, \zeta_2]$  are the improper eigenfunctions. The dispersion relation of any particular magnetic surface  $x_0$  is given by  $\omega^2 = \omega_A^2(x_0, k_y, k_z)$ .

In differential geometric terms, for fixed  $x_0$  the improper eigenfunctions form a line bundle over the base manifold of  $\mathbf{k}$  space. Since these eigenfunctions are not square integrable, there is no clear way to obtain a Berry connection from them, which requires an inner product. Our procedure is first to *regularize* the eigenfunctions with a parameter  $\epsilon$ , giving rise to a regularized line bundle. We then place an inner product on the regularized bundle and determine the Berry connection in the usual way. We shall find that the integral of the Berry curvature of the regularized bundle converges to a value as  $\epsilon \rightarrow 0$ , which we identify with the Chern number of the Alfvén continuum.

We regularize the eigenfunctions by replacing  $s$  with  $s + i\epsilon$ , which is equivalent to a Plemelj form. This regularization has also been used in Alfvén-wave studies of plasma heating [33, 34]. We take  $\epsilon > 0$ . The regularized eigenfunctions are

$$\xi_2(s) = u(s) \ln(s + i\epsilon), \quad (6)$$

$$\eta_2(s) = -\frac{1}{g} \left[ \frac{u(s)}{s + i\epsilon} + u'(s) \ln(s + i\epsilon) \right] + \frac{\hat{g}}{g b^2} u(s) \ln(s + i\epsilon), \quad (7)$$

$$\zeta_2(s) = -\frac{\hat{g}}{f b^2} u(s) \ln(s + i\epsilon), \quad (8)$$

where we have neglected  $v(s)$  because its contributions to the rest of the calculation are subdominant in  $\epsilon$ . We also note that cancellation in Eq. (7) occurs between the third term and part of the second term, after one substitutes the first term in the series for  $u$  and  $u'$ .

We define an inner product

$$\langle \psi | \phi \rangle \stackrel{\text{def}}{=} \int ds h_\epsilon(s) [\xi_\psi^* \xi_\phi + \eta_\psi^* \eta_\phi + \zeta_\psi^* \zeta_\phi], \quad (9)$$

with weight function  $h_\epsilon = \epsilon^2/(\pi(s^2 + \epsilon^4))$ . This weight function has a smaller width than the regularized eigenfunctions, and so effectively acts as a delta function to pick out the behavior on the singular surface at  $s = 0$ .

At this point, we take an explicit model for the magnetic field,  $\mathbf{B}(s) = B_0[(1 + s/L_B)\hat{\mathbf{z}} + s\hat{\mathbf{y}}/L_s]$ . Finite  $L_s$  provides magnetic shear. This model is rather generic

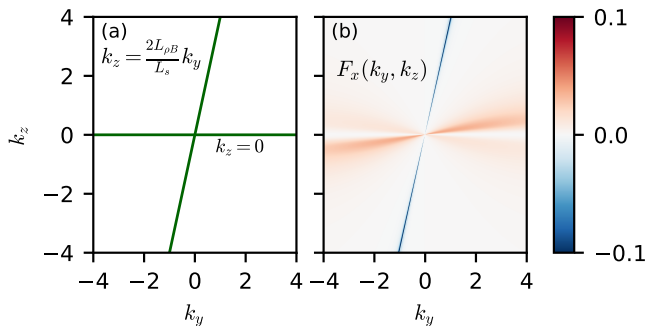


FIG. 1. (a) Lines corresponding to zeros of  $(\omega_A^2)'_0$  in the  $(k_y, k_z)$  plane. (b) Berry curvature  $F_x$ . The Berry curvature is localized near the lines where  $(\omega_A^2)'_0$  is zero. For this figure,  $\epsilon = 0.05$ ,  $L_{\rho B} = 2$ ,  $L_s = 1$ ,  $\hat{g}^2/b_0^4 = 0.6$ , and  $Q_{0a}/B_0^2 = 0.5$ .

for a sheared field within the vicinity of any particular surface, as we may rotate our coordinate system so that  $\hat{\mathbf{z}}$  lies along  $\mathbf{B}(0)$ . The details of the magnetic field enter the rest of the calculation only through  $(\omega_A^2)'_0$ , which is given by

$$(\omega_A^2)'_0 = \frac{B_0^2}{\rho_0} \left( -\frac{1}{L_{\rho B}} k_z^2 + \frac{2}{L_s} k_y k_z \right), \quad (10)$$

where  $1/L_{\rho B} \stackrel{\text{def}}{=} 1/L_\rho - 2/L_B$  and  $L_\rho \stackrel{\text{def}}{=} \rho'_0/\rho_0$ . Figure 1(a) shows the zeros of  $(\omega_A^2)'_0$  in the  $(k_y, k_z)$  plane.

*Berry curvature* Because of the 2-fold degeneracy of the eigenvalue, one must in general consider the non-abelian connection  $\mathcal{A}$  and curvature  $\mathcal{F} = d\mathcal{A} + \mathcal{A} \wedge \mathcal{A}$ . However, the non-singular eigenfunction  $[\xi_1, \eta_1, \zeta_1]$  has zero contribution to the first Chern form, proportional to  $\text{Tr}(\mathcal{F}) = \text{Tr}(d\mathcal{A})$ . To see this, note that the non-singular eigenfunction may be written as real; that is, it does not

change phase with  $\mathbf{k}$ , and hence its diagonal entry in  $\mathcal{A}$  vanishes.

Thus, we need only consider the regularized eigenfunction and its standard Berry connection, given by  $\mathbf{A} = -c_0^{-2} \text{Imag} \langle \psi | \nabla_{\mathbf{k}} \psi \rangle$ , where  $c_0^2 \stackrel{\text{def}}{=} \langle \psi | \psi \rangle$  and  $\nabla_{\mathbf{k}} = \hat{\mathbf{y}} \partial / \partial k_y + \hat{\mathbf{z}} \partial / \partial k_z$ . The localization of the inner product around  $s = 0$  implies we only require  $u(0) = 1$  and  $u'(0) = u_1$  from the Frobenius series, and also picks out  $f(0) = k_z$  and  $g(0) = k_y$ . We find

$$\mathbf{A} = -\frac{\ln \epsilon}{\epsilon} \frac{1}{w} \nabla_{\mathbf{k}} u_{1a}, \quad (11)$$

$$w \stackrel{\text{def}}{=} u_{1a}^2 \ln^2 \epsilon + \left( \frac{1}{\epsilon} - \frac{\pi u_{1a}}{2} \right)^2 + \frac{k_y^2 \hat{g}^2}{k_z^2 b_0^4} \ln^2 \epsilon + k_y^2 \ln^2 \epsilon. \quad (12)$$

Some subdominant terms have been neglected in Eq. (12).

The Berry curvature is given by

$$\mathbf{F} = \nabla_{\mathbf{k}} \times \mathbf{A} = \frac{\ln \epsilon}{\epsilon} \frac{1}{w^2} \nabla_{\mathbf{k}} w \times \nabla_{\mathbf{k}} u_{1a}. \quad (13)$$

It is convenient to evaluate this expression in polar coordinates. Let  $k_y = k \cos \varphi$  and  $k_z = k \sin \varphi$ . We obtain

$$\mathbf{F} = -\hat{\mathbf{x}} \frac{\ln^3 \epsilon}{\epsilon} \frac{1}{w^2} \frac{2Q_{0a}}{B_0^2} \cos^2 \varphi \frac{\frac{2}{L_s} \cos^2 \varphi - \frac{2}{L_{\rho B}} \cos \varphi \sin \varphi}{\left( \frac{2}{L_s} \cos \varphi \sin \varphi - \frac{1}{L_{\rho B}} \sin^2 \varphi \right)^2} \quad (14)$$

Since  $F_x$  is proportional to  $Q_{0a}$ , the Berry curvature vanishes in the absence of gravity. The Berry curvature is shown in Figure 1(b). It is localized near the lines where  $(\omega_A^2)'_0 = 0$ , but the Berry curvature itself does not become singular for finite  $\epsilon$ .

We compute the Chern number as  $C = (2\pi)^{-1} \int d\mathbf{k} F_x$ . After integrating over  $k$  from 0 to  $\infty$ , we obtain

$$C = -\frac{1}{2\pi} \frac{\ln \epsilon}{\epsilon} n_1 \int_0^{2\pi} d\varphi \frac{m_1 \cos^2 \varphi - 2m_2 \cos \varphi \sin \varphi}{[n_1^2 \cos^4 \varphi + n_2^2 \cos^2 \varphi (m_1 \cos \varphi - m_2 \sin \varphi)^2] \ln^2 \epsilon + \left( \frac{\gamma}{\epsilon} - \frac{\pi n_1 \cos^2 \varphi}{2} \right)^2}, \quad (15)$$

where we have defined  $n_1 \stackrel{\text{def}}{=} Q_{0a}/B_0^2$ ,  $n_2 \stackrel{\text{def}}{=} \hat{g}^2/b_0^4$ ,  $m_1 \stackrel{\text{def}}{=} 2/L_s$ ,  $m_2 \stackrel{\text{def}}{=} 1/L_{\rho B}$ , and  $\gamma(\varphi) \stackrel{\text{def}}{=} m_1 \cos \varphi \sin \varphi - m_2 \sin^2 \varphi$ . For small  $\epsilon$ , the dominant contribution arises near the angles where  $\gamma(\varphi)$  vanishes,  $\sin \varphi = 0$  and  $\tan \varphi = m_1/m_2$ . Away from these angles, the  $(\gamma/\epsilon)^2$  term in the denominator is large. These angles are the same as those in which  $(\omega_A^2)'_0 = 0$  and the Frobenius solution of Eq. (4) breaks down. However, these lines are points of measure zero in the area integral and do not pose an impediment to evaluating the integral. Near the peaks where  $\gamma(\varphi)$  vanishes, the integrand can be approx-

imated as a Lorentzian. We obtain, in the limit  $\epsilon \rightarrow 0$ ,

$$C = -\text{sign}(\rho'_0 \hat{g} L_s) \left( 1 - \frac{1}{\sqrt{1 + \frac{4L_s^2}{L_{\rho B}^2}}} \right). \quad (16)$$

The  $\epsilon$  dependence has cancelled out, leaving a finite result. The first term in parentheses in Eq. (16) arises from the  $\tan \varphi = 2L_{\rho B}/L_s$  peaks, while the second term arises from the  $\sin \varphi = 0$  peaks. This ‘‘Chern number’’ is in general not an integer. A non-integer integral of the Berry curvature has been observed in other continuum fluid models to be the result of an insufficiently smooth linear operator at small scales, leading to the inability

to compactify the space [35]. This suggests that regularization of the MHD linear operator at small scales could restore a proper integer Chern number. In the limit of strong magnetic shear,  $L_s \ll L_\rho$ , the second term in the bracket vanishes and  $C = -\text{sign}(\rho'_0 \hat{g} L_s)$ . In the opposite case of weak magnetic shear,  $L_s \gg L_\rho$ , Eq. (16) reduces to the topologically trivial  $C = 0$ .

As additional support for focusing on the first term in parentheses in Eq. (16), we observe that a true Chern number should not change under smooth variations of the inner product. Suppose instead of Eq. (9), we used an alternative inner product, with  $\langle \psi | \phi \rangle = \int ds h_\epsilon(s) [\alpha \xi_\psi^* \xi_\phi + \beta \eta_\psi^* \eta_\phi + \zeta_\psi^* \zeta_\phi]$ , where  $\alpha$  and  $\beta$  are constants. The result for the Chern integral is then modified to be  $C = -\text{sign}(\rho'_0 \hat{g} L_s) (1 - [1 + (4L_\rho^2 / \beta L_s^2)]^{-1/2})$ . Only the second term is affected. Hence, the fact that the result should be independent of  $\alpha$  and  $\beta$  suggests the relative importance of the first term.

The Chern number depends on the sign of the magnetic shear. Therefore, the bulk-boundary correspondence principle implies that a mode will exist localized to a zero-shear layer that separates topologically distinct regions of positive and negative magnetic shear. Figure 2 shows an example in which slab RSAEs are localized to the zero-shear region.

Previous analyses of Eq. (2) in the vicinity of a maximum of  $\omega_A^2$  have revealed a condition for an accumulation point of the discrete spectrum to occur [32]. Let  $x_*$  be the location where  $\omega_A^2(x, k_y, k_z)$  reaches a maximum for given  $k_y, k_z$ . Such a maximum may be created by a minimum in the slab analog of the safety factor,  $B_z(x)/B_y(x)$ . The condition for the maximum of  $\omega_A^2$  to be an accumulation point is  $2(k_y^2 + k_z^2)Q_*/\rho_* |(\omega_A^2)'_*| > 1/4$ , where  $Q_* = -\rho_*' \hat{g}$  and a  $*$  subscript denotes evaluation at  $x_*$ . This condition depends explicitly on the wavevector  $(k_y, k_z)$ . A similar condition arises in a tokamak, with  $Q_*$  replaced by contributions due to energetic particles and toroidicity [8, 9].

In contrast, the topological characterization here provides a different existence condition for interface modes, which only requires nonzero  $\rho' \hat{g}$  and makes no reference to wavevectors. This conclusion is reached only by analyzing the bulk Alfvén continuum away from the region of zero shear. Additionally, the bulk-boundary correspondence principle does not imply the existence of an accumulation point.

Ideal MHD is invariant under an appropriately defined time-reversal transformation in which the magnetic field does not change sign. Such invariance typically implies  $\mathbf{F}(-\mathbf{k}) = -\mathbf{F}(\mathbf{k})$ , and the Berry curvature would therefore integrate to zero. Here, however, the regularization parameter  $\epsilon$  acts like a damping and induces breaking of time-reversal symmetry. The situation is analogous to a Landau damping calculation, in which a symmetry-breaking frequency regularization allows one to recover the Landau damping rate within a Fourier-transform for-

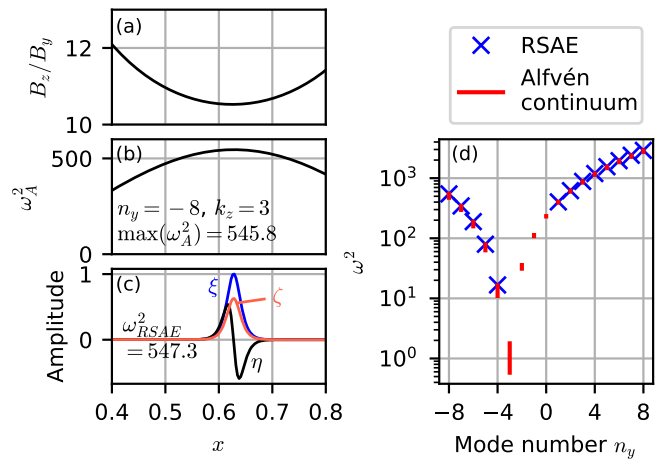


FIG. 2. Slab RSAE spectrum for  $B_z = 5$ ,  $B_y(x) = 1.52x - 1.216x^2$ ,  $\rho(x) = \exp(-x/20)$ ,  $\hat{g} = 75$ . We discretize  $k_y = n_y \Delta k_y$  with  $\Delta k_y = 10$  and integer  $n_y$ , and hold constant  $k_z = 3$ . (a) Safety factor  $B_z(x)/B_y(x)$ , which reaches a minimum at  $x = 0.625$ . (b) Alfvén continuum  $\omega_A^2(x)$  and (c) RSAE eigenfunction at  $n_y = -8$ . (d) RSAE spectrum as a function of  $n_y$ . The fundamental mode is shown, which has eigenvalue  $\omega^2$  larger than the maximum of  $\omega_A^2$ . Solutions with additional spatial nodes may sometimes be found, and have frequency closer to the maximum of the continuum. Also shown is the Alfvén continuum in the interval  $0.5 < x < 0.75$  (outside this interval, the RSAE has little amplitude and would not interact much with the continuum). For  $-3 \leq n_y \leq 0$ , no RSAE is found. In that range,  $\omega_A^2$  inverts and forms a local minimum at  $x \approx 0.625$  instead of a local maximum. To compute the RSAEs, Eq. (1) is solved as an eigenvalue equation with boundary conditions  $\xi(0) = \xi(1) = 0$  using the code Dedalus [36].

malism.

To summarize, in a sheared slab geometry we have associated a nonzero Chern number to the Alfvén continuum on a given magnetic surface, demonstrating that the Alfvén continuum possesses nontrivial topology. The Chern number depends on the sign of the magnetic shear. By appealing to the bulk-boundary correspondence, we expect modes to exist at the interface of zero shear. Our work therefore suggests that reversed-shear Alfvén eigenmodes observed in tokamaks may have topological character. One potential implication is topological robustness of the RSAE in the presence of three-dimensional perturbations such as magnetic islands. Full consideration of the details of toroidal geometry, such as the toroidicity-induced band gaps in the Alfvén continuum spectrum in which the RSAEs reside, are left for future work.

We thank Ian Abel, Vinicius Duarte, Nikolai Gorelenkov, Xian-Zhu Tang for useful discussions. JBP and JBM would like to acknowledge the workshop “Vorticity in the Universe” held at the Aspen Center for Physics in the summer of 2017, which played an important role in bringing about this work. JBP’s work was performed under the auspices of the U.S. Department of Energy

by Lawrence Livermore National Laboratory under Contract No. DE-AC52-07NA27344. JWB's work was supported by the Los Alamos National Laboratory LDRD program under project number 20180756PRD4.

\* [parker68@llnl.gov](mailto:parker68@llnl.gov)

- [1] M. Z. Hasan and C. L. Kane, *Rev. Mod. Phys.* **82**, 3045 (2010).
- [2] L. Lu, J. D. Joannopoulos, and M. Soljačić, *Nat. Photonics* **8**, 821 (2014).
- [3] Z. Yang, F. Gao, X. Shi, X. Lin, Z. Gao, Y. Chong, and B. Zhang, *Phys. Rev. Lett.* **114**, 114301 (2015).
- [4] C. He, X. Ni, H. Ge, X.-C. Sun, Y.-B. Chen, M.-H. Lu, X.-P. Liu, and Y.-F. Chen, *Nat. Phys.* **12**, 1124 (2016).
- [5] R. Süssstrunk and S. D. Huber, *Science* **349**, 47 (2015), <https://science.sciencemag.org/content/349/6243/47.full.pdf>.
- [6] P. Delplace, J. B. Marston, and A. Venaille, *Science* **358**, 1075 (2017), <https://science.sciencemag.org/content/358/6366/1075.full.pdf>.
- [7] M. Perrot, P. Delplace, and A. Venaille, *Nat. Phys.* **15**, 781 (2019).
- [8] H. L. Berk, D. N. Borba, B. N. Breizman, S. D. Pinches, and S. E. Sharapov, *Phys. Rev. Lett.* **87**, 185002 (2001).
- [9] B. N. Breizman, H. L. Berk, M. S. Pekker, S. D. Pinches, and S. E. Sharapov, *Phys. Plasmas* **10**, 3649 (2003), <https://doi.org/10.1063/1.1597495>.
- [10] W. W. Heidbrink, *Phys. Plasmas* **15**, 055501 (2008), <https://doi.org/10.1063/1.2838239>.
- [11] F. Zonca, S. Briguglio, L. Chen, S. Dettrick, G. Fogaccia, D. Testa, and G. Vlad, *Phys. Plasmas* **9**, 4939 (2002), <https://doi.org/10.1063/1.1519241>.
- [12] Y. Kusama, H. Kimura, T. Ozeki, M. Saigusa, G. Kramer, T. Oikawa, S. Moriyama, M. Nemoto, T. Fujita, K. Tobita, G. Fu, R. Nazikian, and C. Cheng, *Nucl. Fusion* **38**, 1215 (1998).
- [13] S. E. Sharapov, B. Alper, H. L. Berk, D. N. Borba, B. N. Breizman, C. D. Challis, A. Fasoli, N. C. Hawkes, T. C. Hender, J. Mailloux, S. D. Pinches, and D. Testa, *Phys. Plasmas* **9**, 2027 (2002), <https://doi.org/10.1063/1.1448346>.
- [14] R. Nazikian, G. J. Kramer, C. Z. Cheng, N. N. Gorelenkov, H. L. Berk, and S. E. Sharapov, *Phys. Rev. Lett.* **91**, 125003 (2003).
- [15] S. E. Sharapov, B. Alper, J. Fessey, N. C. Hawkes, N. P. Young, R. Nazikian, G. J. Kramer, D. N. Borba, S. Haquin, E. De La Luna, S. D. Pinches, J. Rapp, D. Testa, and J.-E. Contributors, *Phys. Rev. Lett.* **93**, 165001 (2004).
- [16] J. A. Snipes, N. Basse, C. Boswell, E. Edlund, A. Fasoli, N. N. Gorelenkov, R. S. Granetz, L. Lin, Y. Lin, R. Parker, M. Porkolab, J. Sears, S. Sharapov, V. Tang, and S. Wukitch, *Phys. Plasmas* **12**, 056102 (2005), <https://doi.org/10.1063/1.1865012>.
- [17] M. Takechi, A. Fukuyama, M. Ishikawa, C. Z. Cheng, K. Shinohara, T. Ozeki, Y. Kusama, S. Takeji, T. Fujita, T. Oikawa, T. Suzuki, N. Oyama, A. Morioka, N. N. Gorelenkov, G. J. Kramer, and R. Nazikian, *Phys. Plasmas* **12**, 082509 (2005), <https://doi.org/10.1063/1.1938973>.
- [18] M. A. Van Zeeland, G. J. Kramer, M. E. Austin, R. L. Boivin, W. W. Heidbrink, M. A. Makowski, G. R. McKee, R. Nazikian, W. M. Solomon, and G. Wang, *Phys. Rev. Lett.* **97**, 135001 (2006).
- [19] E. D. Fredrickson, N. A. Crocker, N. N. Gorelenkov, W. W. Heidbrink, S. Kubota, F. M. Levinton, H. Yuh, J. E. Menard, and R. E. Bell, *Phys. Plasmas* **14**, 102510 (2007), <https://doi.org/10.1063/1.2768038>.
- [20] T. Zhang, H. Liu, G. Li, L. Zeng, Y. Yang, T. Ming, X. Gao, H. Lian, K. Li, Y. Liu, Y. Li, T. Shi, and X. H. and, *Plasma Sci. Technol.* **20**, 115101 (2018).
- [21] K. Toi, F. Watanabe, T. Tokuzawa, K. Ida, S. Morita, T. Ido, A. Shimizu, M. Isobe, K. Ogawa, D. A. Spong, Y. Todo, T. Watari, S. Ohdachi, S. Sakakibara, S. Yamamoto, S. Inagaki, K. Narihara, M. Osakabe, K. Nagaoka, Y. Narushima, K. Y. Watanabe, H. Funaba, M. Goto, K. Ikeda, T. Ito, O. Kaneko, S. Kubo, S. Murakami, T. Minami, J. Miyazawa, Y. Nagayama, M. Nishiura, Y. Oka, R. Sakamoto, T. Shimozuma, Y. Takeiri, K. Tanaka, K. Tsumori, I. Yamada, M. Yoshinuma, K. Kawahata, and A. Komori (LHD Experiment Group), *Phys. Rev. Lett.* **105**, 145003 (2010).
- [22] D. J. Sigmar, C. T. Hsu, R. White, and C. Z. Cheng, *Phys. Fluids B* **4**, 1506 (1992), <https://doi.org/10.1063/1.860061>.
- [23] H. H. Duong, W. W. Heidbrink, E. J. Strait, T. W. Petrie, R. Lee, R. A. Moyer, and J. G. Watkins, *Nucl. Fusion* **33**, 749 (1993).
- [24] M. García-Muñoz, N. Hicks, R. van Voornveld, I. Classen, R. Bilato, V. Bobkov, M. Brambilla, M. Bruedgam, H.-U. Fahrbach, V. Igochine, S. Jaemsae, M. Maraschek, and K. S. and, *Nucl. Fusion* **50**, 084004 (2010).
- [25] D. C. Pace, R. K. Fisher, M. García-Muñoz, W. W. Heidbrink, and M. A. V. Zeeland, *Plasma Phys. Control. Fusion* **53**, 062001 (2011).
- [26] S. E. Sharapov, D. Testa, B. Alper, D. N. Borba, A. Fasoli, N. C. Hawkes, R. F. Heeter, M. Mantsinen, and M. G. V. Hellermann, *Phys. Lett. A* **289**, 127 (2001).
- [27] G. J. Kramer, R. Nazikian, B. Alper, M. de Baar, H. L. Berk, G.-Y. Fu, N. N. Gorelenkov, G. McKee, S. D. Pinches, T. L. Rhodes, S. E. Sharapov, W. M. Solomon, M. A. van Zeeland, and J. E. Contributors, *Phys. Plasmas* **13**, 056104 (2006), <https://doi.org/10.1063/1.2186049>.
- [28] W. Deng, Z. Lin, I. Holod, Z. Wang, Y. Xiao, and H. Zhang, *Nucl. Fusion* **52**, 043006 (2012).
- [29] Y. Chen, T. Munsat, S. E. Parker, W. W. Heidbrink, M. A. Van Zeeland, B. J. Tobias, and C. W. Domier, *Phys. Plasmas* **20**, 012109 (2013), <https://doi.org/10.1063/1.4775776>.
- [30] M. Mathioudakis, D. B. Jess, and R. Erdélyi, *Space Sci. Rev.* **175**, 1 (2013).
- [31] A. J. C. Beliën, S. Poedts, and J. P. Goedbloed, *Phys. Rev. Lett.* **76**, 567 (1996).
- [32] J. P. H. Goedbloed and S. Poedts, *Principles of Magneto-hydrodynamics: With Applications to Laboratory and Astrophysical Plasmas* (Cambridge University Press, 2004).
- [33] A. Hasegawa and L. Chen, *Phys. Rev. Lett.* **32**, 454 (1974).
- [34] L. Chen and A. Hasegawa, *Phys. Fluids* **17**, 1399 (1974), <https://aip.scitation.org/doi/pdf/10.1063/1.1694904>.
- [35] M. G. Silveirinha, *Phys. Rev. B* **92**, 125153 (2015).
- [36] K. J. Burns, G. M. Vasil, J. S. Oishi, D. Lecoanet, and B. P. Brown, Submitted. [arXiv:1905.10388](https://arxiv.org/abs/1905.10388) (2019), (sub-

mitted, [arXiv:1905.10388](#)).